Optimization of Calcium Sulfate Precipitated in the Laminar Flow Pipe through Response Surface Modeling of Temperature, Ca2+ Concentration and Citric acid Additives

by Samsudi Raharjo

Optimization of Calcium Sulfate Precipitated in the Laminar Flow Pipe through Response Surface Modeling of Temperature, Ca^{2+} Concentration and Citric acid Additives

S. RAHARJO[1], S. MURYANTO[2], J. JAMARI[3] and A.P. BAYUSENO[3]*

[1]Department of Mechanical Engineering, Muhammadiyah University in Semarang, Indonesia.
[2]Department of Chemical Engineering, UNTAG University in Semarang, Semarang Indonesia.
[3]Department of Mechanical Engineering, Diponegoro University, Semarang Indonesia.
*Corresponding author E-mail: apbayuseno@gmail.com

ABSTRACT

This paper presents results of investigation of scaling of calcium sulfate ($CaSO_4$) on metallic pipes. In this study, the optimizing variables; namely temperature (50-60°C), concentration of Ca^{2+} (2000-3000 ppm), citric acid concentration (10-20 ppm) were set-up to provide the optimum yield of the mass scales. The mineral scale detected using XRD is mainly gypsum, and the scale has a plate like morphology under SEM examination. SRM (surface response methodology) prediction provided that the temperature is a significant factor, while the Ca^{2+} concentration and the citrate are insignificant variables determining the optimal condition of the mass scale yields. An optimized mass scale response of 119.99 mg was obtained at a temperature of 56.36 °C, concentration Ca^{2+} of 2649.21 ppm and citric acid concentration of 12.11 ppm, respectively. The addition of citric acid did not modify the crystal morphology, but may control the size of crystals.

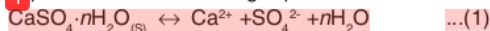Keywords: Calcium sulfate; Surface response methodology (SRM); XRD/SEM analysis; Gypsum.

INTRODUCTION

Calcium sulfate (i.e., gypsum, anhydrite and hemi-hydrate), is commonly formed as scale minerals in pipes of industries ranging from oil and gas to desalination. Scaling of calcium sulfate occurs when the surfaces of metallic pipes contact with the supersaturated water, which can create technological problems such as the diminution of heat transfer, increase of energy consumption and unscheduled equipment shutdown[1-2]. Additionally, this existing scale cannot be removed by acid, but only it can be taken away by mechanical method. Nowadays, much effort has been made in meditating on the precipitation of calcium sulfate in view of their applications in a routine of industrial and environmental engineering[2]. Written report on this mineral scale formation have been previously focused on examining precipitation formed in the bulk solution by using laboratory beaker or bulk jar tests[3].

Here two mechanisms of crystallization of calcium sulfate are commonly experienced in the water system. Firstly, homogenous crystallization frequently occurs in the aqueous solution in the absence of any foreign ions. Secondly, the calcium sulfate particles are mainly formed in heterogeneous processes by the presence of a foreign solid phase[4-5].

Further study on the aspect of calcium sulfate scaling has resulted in numerous studies for the methods to detect and assess the scale formation on metal surfaces. Calcium sulfate has been recognized as a mineral with relative insolubility, thus it can be easy to be precipitated where calcium and sulfate present in the aqueous solution and subsequently lead to the scale formation even at low pH. A theoretical solubility model of the calcium sulfate compounds in water and in multi-component aqueous solutions, has been discussed previously[2]. The solubility of calcium sulfate hydrates may be expressed as the following equation:

$$CaSO_4 \cdot nH_2O_{(S)} \leftrightarrow Ca^{2+} + SO_4^{2-} + nH_2O \qquad ...(1)$$
$$Ca^{2+} + SO_4^{2-} \leftrightarrow CaSO_{4(aq)} \qquad ...(2)$$

where n = 0, 0.5 and 2 corresponding to anhydrite, bassanite and gypsum, respectively. Here, gypsum is considered as the most stable phase found in lower temperatures, while anhydrite can be commonly formed at higher temperatures[6]. Additionally the scale formation of calcium sulfate is influenced by many factors such as concentration of solution, pH value, temperature, pressures, and ionic strength[7]. Correspondingly, sulfate scaling of Ca-ions is of particular interest because this precipitation has shown inverse solubility, *i.e.* its solubility reduces with increasing temperature. Because calcium sulfate polymorphism is a complicating factor, the detailed mineralogical study of deposits is required to understand the mechanism tendency scaling of the surface [6-8].

Mode of scale deposit formation is reported to be classified as two groups[2]: (i) surface crystallization in which mineral precipitated more or less selectively onto the surfaces of the equipment in contact with the aqueous fluids (usually at elevated temperature) and (ii) bulk crystallization which involves the accumulation of precipitates as a result of sedimentation or transport by fluid flow. In this second mode, the scale can be created spontaneously in the bulk, once the supersaturated solution increases, or corrosion by-products are formed at a second stage sediment out. Moreover, scaling in pipe system may be imputed by a combination of these two pathways and also kept in line by the process condition in pipes. Correspondingly, the mitigation of mineral scaling may be performed by the utilization of chemicals and antiscalants for inhibiting nucleation, crystal growth or both. For instance, polyacrylic acid, polyacrylamide, polymaleic anhydride, and polyphosphates are commonly employed [9-10]. At that place are likewise a large number of commercial antiscalants with new formulations being continuously upgraded and tried out for a form of scaling species[7]. Among the various systems of using chemical additives, the prevention of scaling depends on their chemistry and the nature of the solids forming[7]. Here, the use of poly (citric acid) has been demonstrated to suppress the formation of calcium sulfate scale at low concentrations[11]. The poly (citric acid) has the absorption ability of the surface of calcium sulfate scale crystals, thus distorting their scale crystal polymorphs. Therefore, it is potential as a calcium sulfate scale inhibitor, which can be prepared from monomer citric acid. Additionally, the citric acid is usually utilized as additive in the transformation of bassanite to gypsum [12].

Instead, citrate has widely known as scale inhibitor for calcium carbonate (CaCO_3) [13-14-15-16] crystallization, because it can absorb on the calcium carbonate crystal for prevention of crystal particles growing. Nevertheless, a problem of using citric acid in the water system may be linked to the long retention time of crystal growth. Therefore, in that location is still considerable debate and doubt over the mechanism of the effects of variable concentrations of a carboxylic acid and/or various carboxylic acid used in the prevention of crystal growth[17-18]. To come up to this gap results may need a detailed research on the effects of the carboxylic acids (citric, maleic and tartaric) and variable additive concentrations on the kinetics and phase morphologies that develop during calcium sulfate formation reactions and it can subsequently gain a more mechanistic understanding of the crystallization[19].

The present study was undertaken for examining the calcium sulfate scale precipitation in pipes through controlling the independent

operating variables. The variables investigated were: temperature, Ca^{2+} concentration and citric acid additives. Material characterization, including SEM for morphological analysis and XRPD for phase composition was applied in the study. In this work, the central composite design (CCD) for calculating the surface response methodology (SRM), involved temperature and Ca^{2+} concentration, the citric acid additives to maximize calcium sulfate precipitation. A second order transferred polynomial model (as an inverse model) was determined for the yield of mass scale as a function of these variables.

MATERIALS AND METHOD

Reagents

Materials needed in the preparation of the supersaturated solutions were calcium chloride ($CaCl_2$) and sodium sulfate (Na_2SO_4) powder with the analytical grade (Merck™). The citric acid ($C_6H_8O_7$) with analytical grade (Merck™) was also used as additives. The crystal-forming solutions were made using distilled water.

Procedures and measurements

Experiments were carried out using a laboratory equipment for calcium sulfate crystallization is shown in Fig. 1. Crystallization experiments were performed similar to the method proposed by Muryanto *et al* (2014)[20], by dissolving each of $CaCl_2$ and Na_2SO_4 crystals in the distilled water (500 ml) for providing Ca^{2+} concentration of 2000, 2500 and 3000 ppm. Citric acid (10, 15 and 20 ppm) was added by dissolving the crystals $C_6H_8O_7$ in a vessel containing 500 ml of solution $CaCl_2$, then stirred until well mixed. For the experiment, one liter containing each of equimolar $CaCl_2$ and Na_2SO_4 was prepared. The solutions at predetermined concentrations were separately placed in the two vessels and equilibrated until the designated temperature (50-60 $^{\circ}$C) was reached. The conductivity of solutions, leaving the test pipe section was continuously checked for up to 2 hours. The scale deposited on the surface of the coupons within the housing sample was carefully removed and dried in an oven overnight at 60 $^{\circ}$C. The dried coupons were taken out to be weighed. The weight difference of the coupons obtained before and after the experiments was identified as the scale mass. The scale deposited on the surface of the coupons was carefully removed and kept in a plastic container for subsequent characterization.

Materials characterization

All powder samples were carbon-coated prior to investigation by scanning electron microscopy (SEM) (FEI Inspect S50) with energy dispersive spectroscopy (EDS) system fitted with a field emission source and operating at an accelerating voltage of 15 KV. Phase identification of scale mineral was conducted by XRPD (X-ray powder diffraction) analysis. XRPD data were acquired by a conventional Bragg-Brentano (BB) diffractometry with parafocusing geometry and Cu-Ká monochromated radiation. The scan parameters (5-90 2è$^{\circ}$, 0.020 steps, 15 s/step) were taken as required for observation. A PC-based search match program, the Philips X'Pert Software (Philips Electronics N.V) was to identify possible crystalline phases in the samples. In this method, the peak positions and peak heights were verified against the entries in the ICDD-PDF (International Centre for Diffraction Data-Powder Diffraction File). The identified mineral phases were subsequently adjusted by Rietveld method using Fullprof-2k, software, program version 3.30 [21-22]. The crystal structure model for the Rietveld refinement was obtained in the AMCSD (American Mineralogist crystal structure database). The detailed discussion of the method is provided elsewhere [23-24].

Experimental design

In this study, the optimization of the three variables (temperature, Ca^{2+} concentration, and citric acid) to yield the optimum mass scale was performed using SRM within the CCD (Table 1). SRM calculation was conducted by the statistical v. 6 software packages (StatSoft, Tulsa, OK, USA). Using this method, the proper response value and mathematical model fitted to the measured data was acquired from the experiments, and the independent variables of optimal conditions.

RESULTS AND DISCUSSION

Properties of solid precipitated crystals

The corresponding solid crystals were subjected to XRPD as shown in Figures 2a and 2b. The quality of Rietveld refinements of the crystalline scale may be gained from the diffraction plot (Fig. 2a), where the assigned phases clearly stand out in the difference curve of the calculated and the

measured diffraction profile. The Rietveld analysis of crystals proved that only the gypsum polymorph present in scale obtained from the solution in the absence of additives at a temperature of 50 $^\circ$C. In this experiment, metastable crystalline phases of bassanite and amorphous calcium sulfate were not identified. Depending on the amount of citric acid additives, gypsum crystals were predominantly precipitated on the surface of all coupon samples (Fig. 2b). Nevertheless, in the presence of 10 ppm citric acid additive, it is shown that the probability amorphous phase of calcium sulfate, which have peaks with low intensity, could be identified by their XRPD patterns.

Further, gypsum crystal habit, morphology and size did not vary throughout the sample depth depending on the additive concentration. The surface of gypsum crystals was composed of micrometer-sized monoclinic crystals with a plate-like morphology (Fig. 3). This gypsum crystals are same as the finding in the literature[18]. These crystals formed a layer at the surface within a size of around 10 µm (Fig. 3a-c). In the presence of 20 ppm citric acid, the shape, size or habit of the end-product gypsum were similar to the CaSO4 experiment without additives, although several small size of the gypsum needles was observed. The citric acid additive may control the growth of the scale mineral, however, there was no

Table 1: Range and level of independent variable

Independent variable	Range and level		
	Low level (-1)	Center level (0)	High level (+1)
Temperature ($^\circ$C)	50	55	60
Concentration Ca^{2+} (ppm)	2000	2500	3000
Citric acid (ppm)	10	15	20

Table 2: Factor and level for SRM and experimental design with independent variables

Run	Independent variable			Response
	Temperature ($^\circ$C)	Concentration Ca^{2+} (ppm)	Citric Acid (ppm)	Mass scales (mg)
1	50.00	2000.00	10.00	44
2	50.00	2000.00	20.00	35
3	50.00	3000.00	10.00	88
4	50.00	3000.00	20.00	25
5	60.00	2000.00	10.00	64
6	60.00	2000.00	20.00	75
7	60.00	3000.00	10.00	86
8	60.00	3000.00	20.00	102
9	46.59	1500.00	15.00	15
10	63.41	1500.00	15.00	118
11	55.00	659.10	15.00	11
12	55.00	2340.90	15.00	87
13	55.00	1500.00	6.59	88
14	55.00	1500.00	23.41	13
15 (C)	55.00	1500.00	15.00	82
16 (C)	55.00	1500.00	15.00	82

significant different habits found in gypsum obtained from the solution to the free-additive.

Predicted model and statistical analysis

Variables for response optimization was modeled using SRM with the CCD (Table 1), where there are 3 factorial design $2^{(3)}$ in CCD providing nc = 8; ns = 6; no = 2 and run = 16. Moreover preliminary studies were carried out to determine the required range of temperatures (X_1, 50-60 °C),

Ca^{2+} concentration (X_2, 1500-3000 ppm) and citric acid additives (X_3, 10 -20 ppm). Factors and level for SRM consisted of low level (-1) = 50; 2000; 10, high level (+1) = 60; 3000; 20, and center point (0) = 55; 2500; 15. The whole design of experimental response of mass scales (mg) is listed in Table 2.

Based on multiple regression analysis of the experimental data, the optimization resulted in the following second-order polynomial equation in term of code values:
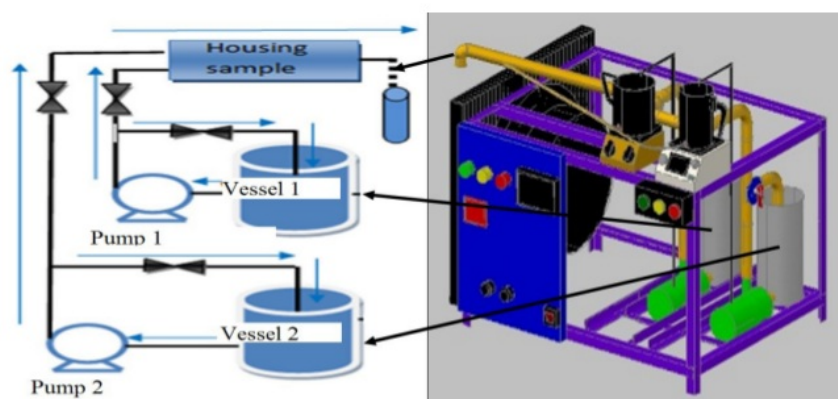

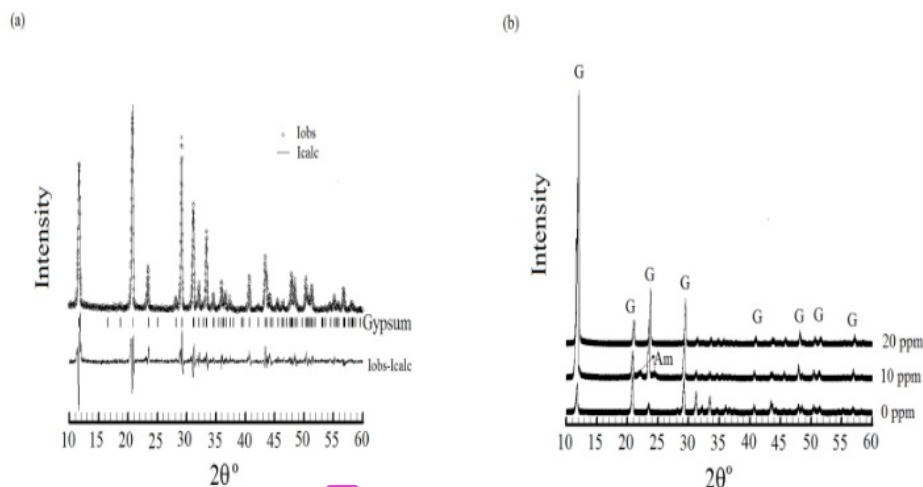**Fig. 1: Schematics of equipment used for calcium sulfate scale formation in pipes**

Fig. 2: (a) Plot of XRPD Rietveld analysis of the scale crystals precipitated in the solution of 2000 ppm Ca^{2+} concentration without additive at a temperature of 50 °C; (b) XRPD pattern of the crystals obtained from the solution in the presence of various citric acid at a temperature of 50 °C. Here, G (gypsum) and Am (amorphous) is noted

$Y = -452.9011 + 15.24867\, X_1 - 0.03793\, X_1{}^2 + 0.0868\, X_2 + 0.000002\, X_2{}^2 - 21.21898\, X_3 + 0.3642\, X_3{}^2 - 0.00143\, X_1X_2 + 0.495\, X_1X_3 - 0.00116\, X_2X_3$

where Y is the yield of mass scale (mg), and X_1, X_2 and X_3 are the coded variables for temperature, Ca^{2+} concentration and citric acid concentration, respectively. Analysis of variance (ANOVA) for the statistical testing of the model is shown in Table 3. Here, the ANOVA fitted the quadratic polynomial model of mass scale yield. The influence of the significance of a factor can be seen from F-value

and p-value. The quadratic regression model showed the value of determination coefficient (R^2) of 0.965 with no significant lack of fit at $p > 0.05$ which means that the calculated model fitted 96.5 % of the result and only 3.5% of the total variation did not fit to the model. The p-value less than 0.05 with an accuracy of 95% indicates that the relationship between the response and the independent variables can be fitted using the model. The significance of the model was also judged by F-test, where F -value is defined as the ratio between MSF (mean squares of factor) of
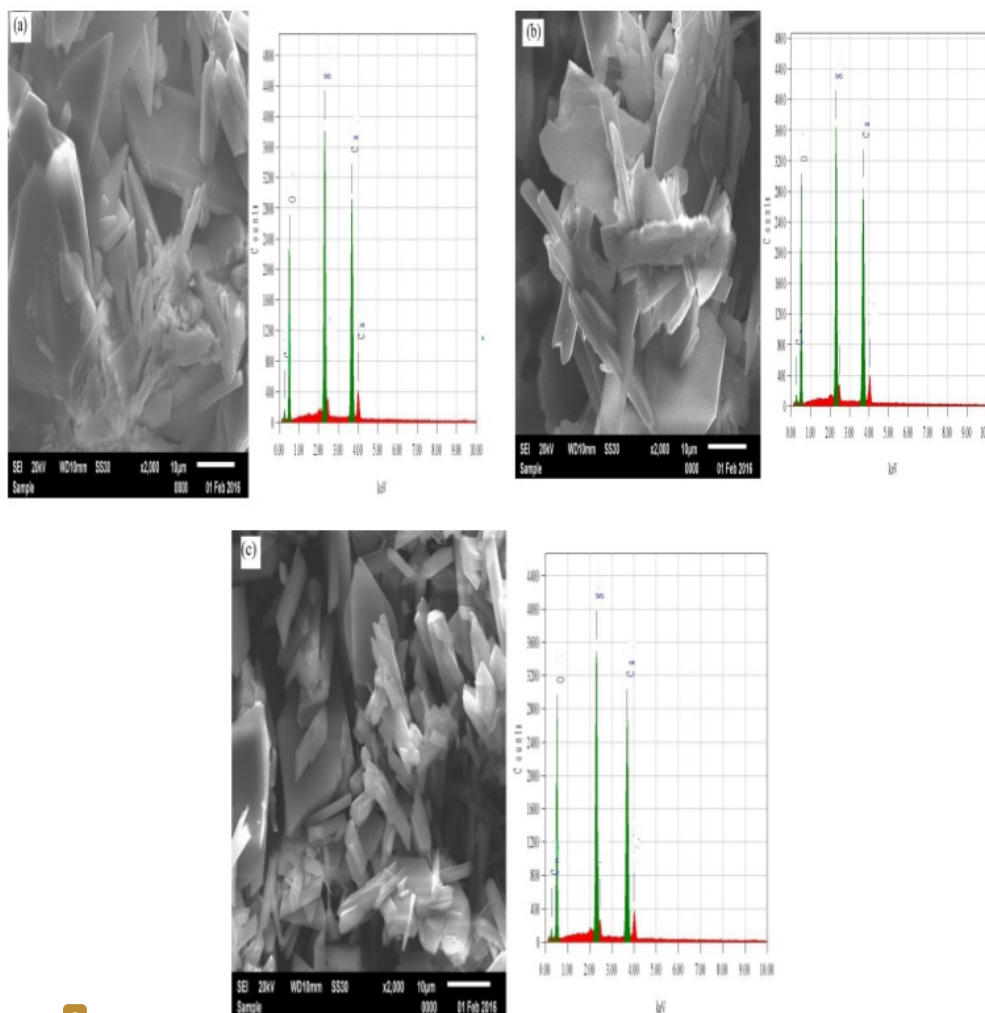

Fig. 3: Morphology of the calcium sulfate precipitated in the solution of 2000 ppm Ca^{2+} concentration with; a) 0 ppm; b) 10 ppm and c) 20 ppm citric acid additives and temperature of 50 °C

the MSE (mean squares of error). A factor can be said to have a significant effect when the *F*-value is greater than *F*-table.

The *F*-value of model compared with the *F*-table shown in Table 3, provided that the *F*-value is greater than the *F*- table. This demonstrates a substantial outcome on the response variable of the mass scales. The same matter can be seen in chart Pareto, as depicted in Figure 4.

It shows that *p*-value is less than 0.05 providing that the independent variables have insignificant effect. Apparently, the optimization variables for the response of the scale mass (mg)

may be related to the temperature (X_1). In contrast, the influence of linear concentration (X_2), linear of citric acid (X_2), the interaction between temperature and citric acid ($X_1 X_3$), quadratic concentration (X_2^2), quadratic of citric acid (X_3^2), the interaction between temperature and concentration ($X_1 X_2$), the interaction and the concentration of citric acid ($X_1 X_2$), quadratic temperature (X_1^2) can be ignored because they may not provide a significant effect on the response of the mass scales.

Optimization of independent variables for the response of mass scale

The interaction of independent variables in response of mass scale yield was depicted by 3D

Table 3: ANOVA for the fitted quadratic polynomial model of yield of mass scale

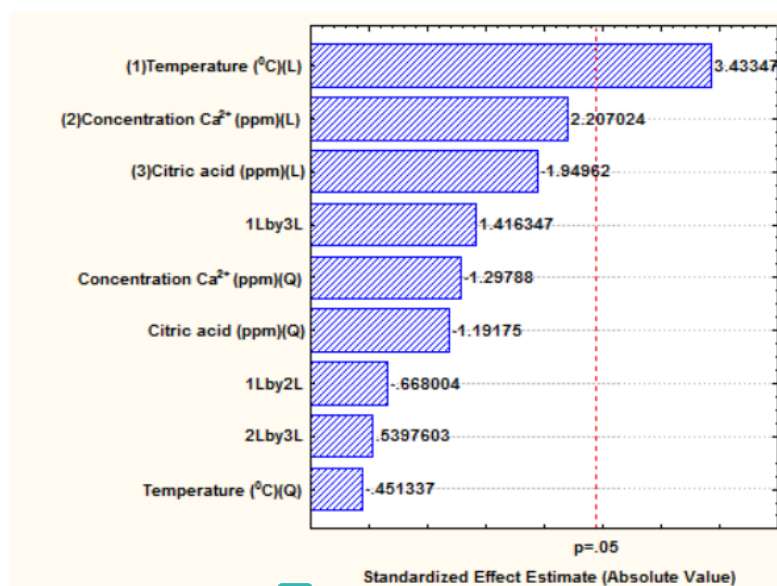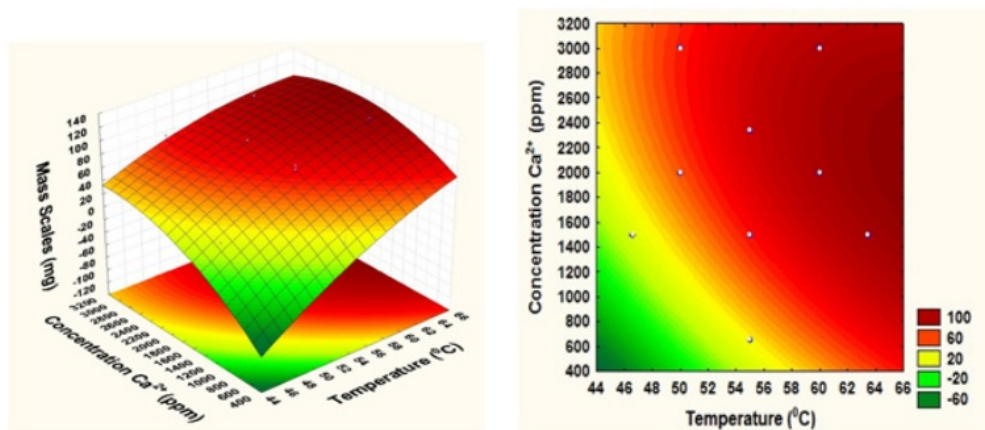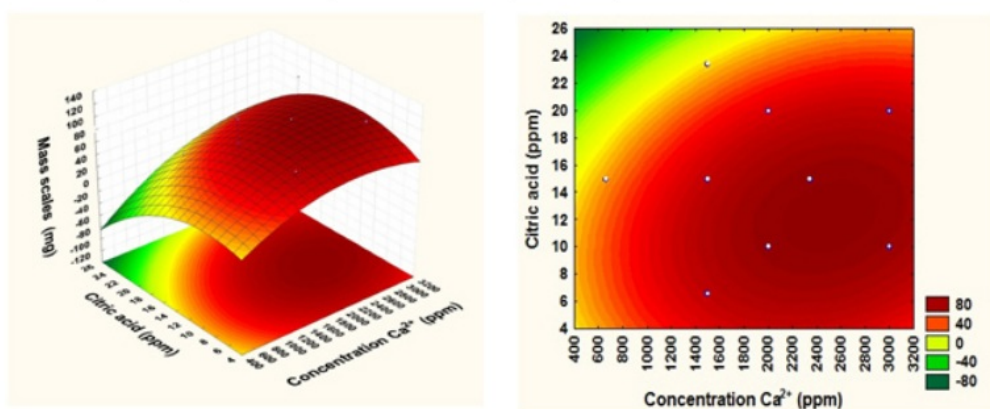| Source	Sum of Squares (SS)	Degree of freedom (DF)	Mean Square (MS)	*F*-value	*F*-table	R²
S.S. regression	16191.88	9	16191.88	26.51	4.1	0.965
S.S. error	3664.31	6	610.719			
S.S. Total	19856.19	15				

Fig. 4: Pareto chart of optimization independent variables on the response of the mass scales (mg)

Fig. 5: Response surface plot and contour plot of temperature and Ca²⁺ concentration

Fig. 6: Response surface plot and contour plot of citric acid and Ca²⁺ concentration
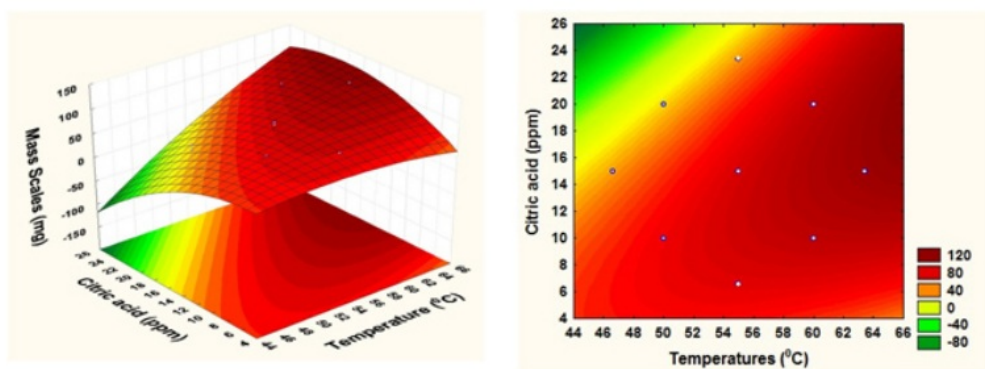
Fig. 7: Response surface plot and contour plot of citric acid and temperatures

Table 4: Optimum mass scales

Factor	Optimum state	Optimum mass scales (mg)
Temperature ($^{\circ}$C)	56.36	119.99
Concentration Ca^{2+} (ppm)	2649.21	
Citric acid (ppm)	12.11	

Table 5: Optimum conditions and the predicted and experimental value of response at the optimum conditions

Optimal variable	Optimum Result SRM Mass scales	Experiment Result	% Relative Error
Temperatures ($^{\circ}$C)	56.36	119.99	121.34	1.11 %
Concentration Ca^{2+} (ppm)	2649.21			
Citric acid (ppm)	12.11			

Relative error (%) = [(Experimental result − Optimum result SRM)/Experimental result] × 100%.

response surface and 2D contour plots created by the model (Figs. 5-7). Different shapes of the contour plots showed different interactions between the variables, where the significant interactions between the variables was represented as an elliptical contour plot. In contrast, a circular contour plot presents the insignificant relationships between independent and dependent variables. Fig. 5 presents the interaction between temperature (X_1) and Ca^{2+} concentration (X_2) on the yield of mass scale. When the temperature below 50 $^{\circ}$C, there was a small amount in the response, and the temperature below 50 $^{\circ}$C did not show any obvious effect on extraction yield. However, the increase of temperature from 50 to 66 $^{\circ}$C make improve the mass scale yield. The possible explanation could be that the increase in temperature can increase reaction speed and collisions between molecules occurring more quickly, so that the mass scale formation increases[25].

Fig. 6 describes the effect of Ca^{2+} concentration (X_2) and additive concentration (X_3) on the yield of mass scale. It can be observed that when Ca^{2+} concentration (X_2) was fixed at 0 levels, additive concentration (X_3) displayed a quadratic effect on the response yield. Varying Ca^{2+} concentration from 1500 to 3000 ppm with an increase of citric acid additives from 8 to 16 ppm, the target compounds' mass scale yield was increasing with increase of Ca^{2+} concentration. Fig. 7 illustrates that an increase in temperature (X_1) leads to increased production of mass scale. Maximal mass scale production was obtained at a citric acid concentration (X_3) of 12.11 ppm. Here, the optimal range for mass scale production was from 50 to 66 $^{\circ}$C and citrate of 10 to 20 ppm.

To determine the optimum mass scales was done by entering values   into the equation, which include the optimum ratio of the mass response for variable optimization. Optimum mass scales are shown in Table 4.

Validation of the predicted value for the optimal variable

The results of SRM optimization were then verified using the experimental data. Verification was conducted by comparing the results of SRM optimization with the results of laboratory experiments. The calculation generated to the optimum yields of mass scale was based on temperatures (56.36 $^{\circ}$C), Ca^{2+} concentration (2649.21 ppm) and citric acid additives (12.11 ppm), respectively. As shown in Table 4, three

parallel experiments were carried out under the optimal conditions. The software predicted that the precipitated yield of total mass scale was 119.99 mg. The comparison was performed to acquire the % error of difference in optimizing response. Table 5 present results of experiments conducted in conformity with the optimum ratio of SRM for analysis yielding the mass scale of 121.34 mg. From the results of these experiments, the % error was calculated. Here the calculated % error for the mass scale response was 1.11 %. This means for the mass scale response has an accuracy of 99.99 %. So the results of the SRM optimization analysis were in agreement with the data of experimental mass scales.

CONCLUSIONS

SRM optimization of variable operating conditions, provided that the most influence on the mass of the scale is temperature. The optimum result

with the mass response scale (119.99 mg) was related to temperature of 56.36 °C; concentration Ca^{2+} of 2649.21 ppm; citric acid of 12.11ppm, respectively. The crystalline phase of the scale was found to be mostly gypsum as shown by the XRD, although the amorphous phase may be developed on the scale in the solution with 10 ppm additive and a temperature of 50 °C. The SEM analysis also showed that the scale has a plate like morphology. The addition of citric acid seemed to not change the crystal morphology, only the possibility of citric acid additives may control crystal growth on the surface of the particles.

ACKNOWLEDGMENTS

REFERENCES

1. Al Nassera, W.N.; Al-Salhib, F.H.; Hounslowa, M.J.; Salmana, A.D. *Chem. Eng. Res. Des.* **2011**, *89*, 500-511
2. Azimi, G.; Papangelakis, V.G.; Dutrizac. J.E. *Fluid Phase Equilibr.* **2007**, *260*, 300-315
3. Amiri, M.; Moghadasi, J. *Pet. Sci. Technol.* **2012**, *30*, 223-236
4. Benatti, C.T.; Tavares, C.R.G.; Lenzi, E. *J. Environ. Manage.* **2009**, *90*, 504-511
5. Silva, R.; Cadorin, L.; Rubio, J. *Miner. Eng.* **2010**, *23*, 1220-1226
6. Singh, N.B.; Middendorf, B. *Prog. Cryst. Growth Ch.* **2007**, *53*, 57-77
7. Amjad, Z.; Koutsoukos, P.G. *Desalination.* **2014**, *335*, 55–63
8. Camarini, G.; De Milito, J.A. *Constr. Build. Mater.* **2011**, *25*, 412- 4125
9. Kavitha, A.L.; Vasudevan, T.; Prabu, H.G. *Desalination.* **2011**, *268*, 38-45
10. Wang, C.; Zhu, D.; Wang, X. *J. Appl. Polym. Sci.* **2010**, *115*, 2149-2155
11. Zhao, Y.; Jia, L.; Liu, K.; Gao, P.; Ge, H.; Fu, L. *Desalination.* **2016**, *392*, 1-7
12. Saha, A.; Lee, J.; Pancera, S.M. *Langmuir.* **2012**, *28*, 11182-11187
13. Bassioni, G. *J. Pet. Sci. Eng.* **2010**, *70*, 298-301.
14. Chaussemier, M.; Pourmohtasham, E.; Gelus, *Desalination.* **2015**, *356*, 47-55
15. Al-Roomi, Y.M.; Hussain, K.F. *Desalination.* **2016**, *393*, 186-195
16. Kýrboga, S.; Öner, M. *Colloid. Surface. B.* **2012**, *91*, 18-25
17. Hasson, D.; Shemer, H.; Sher, A. *Ind. Eng. Chem. Res.* **2011**, *50*, 7601-7607
18. Rabizadeh, T.; Peacock, L. C.; Benning, L.B. *Mineral. Mag.* **2014**, *78*, 1465-1472
19. Tzotzi, C.; Pahiadaki, T.; Yiantsios, S.G.; Karabelas, A.J.; Andritsos, N. *J Mater. Sci.* **2007**, *296*, 171-184
20. Muryanto, S.; Bayuseno, A.P.; Sediono, W.; Mangestiyono, W. *Education for Chemical Engineers.* **2012**, *7*, 78-84
21. Rietveld H.M. *J. Appl. Crystallogr.* **1969**, *2*, 65-71
22. Rodriguez-Carvajal J. Program Fullprof.2k, version 3.30, Laboratoire Leon Brillouin, France, June **2005**.
23. Bayuseno A.P.; Schmahl W.W. *Int. J. Environ. Waste Manage.* **2015**, *15*, 39-66
24. Mahieux P.-Y.; Aubert J.-E.; Cyr M.; Coutand, M.; Husson B. *Waste Manage.* **2010**, *30*, 378-388
25. Martinod, A.; Euvrard, M.; Foissy, A.; Neville, A. *Desalination.* **2007**, *220*, 345-352

Optimization of Calcium Sulfate Precipitated in the Laminar Flow Pipe through Response Surface Modeling of Temperature, Ca2+ Concentration and Citric acid Additives

6   F. Sariman, A.P. Bayuseno, S. Muryanto. " Crystallization of Barium Sulfate (BaSO) in a Flowing System: Influence of malic acid on Induction Time and Crystal Phase Transformation ", MATEC Web of Conferences, 2018
Publication

1 %

7   Bayuseno, A.P.. "Characterization of MSWI fly ash through mineralogy and water extraction", Resources, Conservation & Recycling, 201103
Publication

1 %

8   Pouralinazar, F.. "Pressurized liquid extraction of Orthosiphon stamineus oil: Experimental and modeling studies", The Journal of Supercritical Fluids, 201202
Publication

<1 %

9   Jolanta Latosińska, Jarosław Gawdzik. "The Impact of Combustion Technology of Sewage Sludge on Mobility of Heavy Metals in Sewage Sludge Ash/Wpływ Technologii Spalania Komunalnych Osadów Ściekowych Na Mobilność Metali Ciężkich Z Popiołów", Ecological Chemistry and Engineering S, 2014
Publication

<1 %

10 Curcio, Efrem, Vilmalí López-Mejías, Gianluca Di Profio, Enrica Fontananova, Enrico Drioli, Bernhardt L. Trout, and Allan S. Myerson.

<1 %

"Regulating Nucleation Kinetics through Molecular Interactions at the Polymer–Solute Interface", Crystal Growth & Design, 2014.
Publication

11   Jie PENG, Xin-zhi LIU, Fu-li GUO, Song-bai HAN, Yun-tao LIU, Dong-feng CHEN, Xin-hua ZHAO, Zhong-bo HU. "Crystal structure and negative thermal expansion properties of solid solution Er2W3−xMoxO12", Transactions of Nonferrous Metals Society of China, 2009
Publication
<1 %

12   Cojocaru, C.. "Response surface modeling and optimization of copper removal from aqua solutions using polymer assisted ultrafiltration", Journal of Membrane Science, 20070720
Publication
<1 %

13   Submitted to University of Wales, Bangor
Student Paper
<1 %

14   Taher Rabizadeh, Tomasz M. Stawski, David J. Morgan, Caroline L. Peacock, Liane G. Benning. "The Effects of Inorganic Additives on the Nucleation and Growth Kinetics of Calcium Sulfate Dihydrate Crystals", Crystal Growth & Design, 2017
Publication
<1 %

15   A.P. Bayuseno, W.W. Schmahl, Th. Müllejans. "Hydrothermal processing of MSWI Fly Ash-
<1 %

towards new stable minerals and fixation of heavy metals", Journal of Hazardous Materials, 2009
Publication

16 www.publish.csiro.au
Internet Source
<1 %

17 Moyer, Bruce A., Radu Custelcean, Benjamin P. Hay, Jonathan L. Sessler, Kristin Bowman-James, Victor W. Day, and Sung-Ok Kang. "A Case for Molecular Recognition in Nuclear Separations: Sulfate Separation from Nuclear Wastes", Inorganic Chemistry, 2012.
Publication
<1 %

18 Qi Wang. "Response Surface Methodology Analysis of Biodegradation of Acrylonitrile in Bioreactor", Communications in Computer and Information Science, 2011
Publication
<1 %

19 M. S. Shalaby. "Modeling and Optimization of Phosphate Recovery from Industrial Wastewater and Precipitation of Solid Fertilizer using Experimental Design Methodology", Chemical and Biochemical Engineering Quarterly Journal, 2015
Publication
<1 %

20 hal-insu.archives-ouvertes.fr
Internet Source
<1 %

21 Jiang, Man, Guangsong Chen, Ping Lu, and Jian Dong. "Preparation of aqueous soluble polyamides from renewable succinic acid and citric acid as a new approach to design bio-inspired polymers", Journal of Applied Polymer Science, 2014.
Publication

<1%

22 Tianzhen Zhu, Lida Wang, Wen Sun, Zhengqing Yang, Suilin Wang, Yingzheng Zhou, Shaohui He, Yaowei Wang, Guichang Liu. "Corrosion-Induced Performance Degradation of Phosphorus-Containing Scale Inhibitors at Carbon Steel–Water Interface", Industrial & Engineering Chemistry Research, 2018
Publication

<1%

23 sinta3.ristekdikti.go.id
Internet Source

<1%

24 Zhang, Huixin, Zhiyue Cai, Xiuhong Jin, Dongxue Sun, Dongdong Wang, Tingru Yang, Jie Zhang, and Xu Han. "Preparation of modified oligochitosan and evaluation of its scale inhibition and fluorescence properties", Journal of Applied Polymer Science, 2015.
Publication

<1%

25 Submitted to Universidad San Francisco de Quito
Student Paper

<1%

26 Submitted to Rutgers University, New Brunswick
Student Paper
<1%

27 S. Sutiyono, Luluk Edahwati, Dyah Suci Perwitasari, Stefanus Muryanto, J. Jamari, Anatasius P. Bayuseno. "Synthesis and Characterisation of Struvite Family Crystals by An Aqueous Precipitation Method", MATEC Web of Conferences, 2016
Publication
<1%

28 link.springer.com
Internet Source
<1%

29 www.beilstein-journals.org
Internet Source
<1%

30 Preston R. Larson, Andrew S. Madden, A. Cuneyt Tas. "Non-stirred synthesis of Na- and Mg-doped, carbonated apatitic calcium phosphate", Ceramics International, 2013
Publication
<1%

31 Xiaoyu Sun, Junping Zhang, Chengxian Yin, Juantao Zhang, Jiao Han. "Poly(aspartic acid)-tryptophan grafted copolymer and its scale-inhibition performance", Journal of Applied Polymer Science, 2015
Publication
<1%

32 Liu, J.. "Optimization of the enzymatic pretreatment in oat bran protein extraction by
<1%

particle swarm optimization algorithms for response surface modeling", LWT - Food Science and Technology, 200812
Publication

---

33 Carmona, N.. "Optical sensors for evaluating environmental acidity in the preventive conservation of historical objects", Sensors & Actuators: A. Physical, 20041029
Publication

<1%

---

34 hdl.handle.net
Internet Source

<1%

---

35 Syed Taha Taqvi, Ali Almansoori, Ghada Bassioni. "Understanding the Role of Asphaltene in Wettability Alteration Using ζ Potential Measurements", Energy & Fuels, 2016
Publication

<1%

---

36 wrap.warwick.ac.uk
Internet Source

<1%

---

37 Submitted to University of Sheffield
Student Paper

<1%

---

38 Submitted to Universiti Teknologi Malaysia
Student Paper

<1%

---

39 www.mater-rep.com
Internet Source

<1%

---

40 Khayet, M.. "Response surface modelling and

<1%

optimization in pervaporation", Journal of Membrane Science, 20080815
Publication

41 Submitted to Gyeongsang National University
Student Paper
<1%

42 Azam Hajizadeh, Tayebe Bagheri Lotfabad, Manochehr Bahmaei. "Assessment of aqueous extract of Gypsophila aretioides for inhibitory effects on calcium carbonate formation", Green Processing and Synthesis, 2019
Publication
<1%

43 Joiret, Suzanne, Françoise Pillier, and Annie Lemarchand. "Submicrometric Picture of Plaster Hydration: Dynamic and Space-Resolved Raman Spectroscopy versus Kinetic Monte Carlo Simulations", The Journal of Physical Chemistry C
Publication
<1%

44 Submitted to Pukyong National University
Student Paper
<1%

45 Saidina Amin, N.A.. "SCR of NO with C"3H"6 in the presence of excess O"2 over Cu/Ag/CeO"2-ZrO"2 catalyst", Chemical Engineering Journal, 20051001
Publication
<1%

46 Onay Burak Dogan, Baran Onal-Ulusoy, Faruk Bozoglu, Adviye Gulcin Sagdicoglu-Celep,
<1%

Deniz Cekmecelioglu. "Detoxification of Groundnut Cake Naturally Contaminated with Aflatoxin B1 Using Rhodococcus erythropolis in Shake Flask Bioreactors", Waste and Biomass Valorization, 2016
Publication

47   R. O. Cristóvão, A. P. M. Tavares, J. M. Loureiro, R. A. R. Boaventura, E. A. Macedo. "OPTIMISATION OF REACTIVE DYE DEGRADATION BY LACCASE USING BOX–BEHNKEN DESIGN", Environmental Technology, 2008   <1%
Publication

48   Shen, Q.. "Morphological control of calcium carbonate crystals by polyvinylpyrrolidone and sodium dodecyl benzene sulfonate", Colloids and Surfaces A: Physicochemical and Engineering Aspects, 20041220   <1%
Publication

49   Submitted to iGroup   <1%
Student Paper

50   Ali Mirzaalian Dastjerdi, Zahra Kargozarfard, Bita Najafi, Vahid Taghikhani, Shahab Ayatollahi. "Microscopic Insight into Kinetics of Inorganic Scale Deposition during Smart Water Injection Using Dynamic Quartz Crystal Microbalance and Molecular Dynamics   <1%

Simulation", Industrial & Engineering Chemistry
Research, 2019
Publication

51	www.aquamem.com Internet Source	<1%

52	Submitted to Universiti Putra Malaysia Student Paper	<1%

Exclude quotes	Off	Exclude matches	< 1 words
Exclude bibliography	Off		